Available online at www.sciencedirect.com

SCIENCE DIRECT

Life Sciences 78 (2006) 2633 – 2642

Life Sciences

www.elsevier.com/locate/lifescie

Acute changes of biventricular gene expression in volume and right ventricular pressure overload

Roberto Roncon-Albuquerque Jr., Mariana Vasconcelos, André P. Lourenço, Ana Brandão-Nogueira, Antónia Teles, Tiago Henriques-Coelho, Adelino F. Leite-Moreira *

Department of Physiology, Faculty of Medicine of Porto, Porto, Portugal

Received 2 April 2005; accepted 12 October 2005

Abstract

Objective: We investigated the effects of acute volume and RV pressure overload on biventricular function and gene expression of BNP, pro-inflammatory cytokines (IL-6 and TNF-α), iNOS, growth factors (IGF-1, ppET-1), ACE and Ca^{2+}-handling proteins (SERCA2a, phospholamban and calsequestrin).

Methods: Male Wistar rats ($n=45$) instrumented with pressure tip micromanometers in right (RV) and left ventricular (LV) cavities were assigned to one of three protocols: i) Acute RV pressure overload induced by pulmonary trunk banding in order to double RV peak systolic pressure, during 120 or 360 min; ii) acute volume overload induced by dextran40 infusion (5 ml/h), during 120 or 360 min; iii) Sham. RV and LV samples were collected for mRNA quantification.

Results: BNP upregulation was restricted to the overloaded ventricles. TNF-α, IL-6, ppET-1, SERCA2a and phospholamban gene activation was higher in volume than in pressure overload. IGF-1 overexpression was similar in both types of overload, but was limited to the RV. TNF-α and CSQ mRNA levels were increased in the non-overloaded LV after pulmonary trunk banding. No significant changes were detected in ACE or iNOS expression. RV end-diastolic pressures positively correlated with local expression of BNP, TNF-α, IL-6, IGF-1, ppET-1 and SERCA2a, while RV peak systolic pressures correlated only with local expression of IL-6, IGF-1 and ppET-1.

Conclusions: Acute cardiac overload alters myocardial gene expression profile, distinctly in volume and pressure overload. These changes correlate more closely with diastolic than with systolic load. Nonetheless, gene activation is also present in the non-overloaded LV of selectively RV overloaded hearts.

Keywords: Gene expression; Growth factors; Hemodynamics; Mechanotransduction

Introduction

Cardiac overload is one of the most important stimuli for heart failure progression (Hoshijima and Chien, 2002; Sussman et al., 2002). In this disease, chronic activation of growth promoting signals induces both hypertrophy and a shift in the gene expression profile of terminally differentiated cardiomyocytes. Changes in the transcription program include regression to the molecular fetal phenotype, upregulation of pro-inflammatory cytokines and growth factors, and disturbed expression of Ca^{2+}-handling genes. Although hypertrophy contributes, at least in the early phases of heart failure progression, to ventricular function preservation, the shift in myocardial gene expression profile has been associated with the main end-points of the disease, namely contractile dysfunction, cardiomyocyte apoptosis and necrosis, myocardial fibrosis and arrythmogenesis (Morisco et al., 2003).

Despite extensive knowledge on the molecular mechanisms of myocardial hypertrophy, much less is known about the acute response to cardiac overload. There is, however, growing evidence for disturbed cardiomyocyte gene expression profile. Pikkarainen et al. observed increased type-B natriuretic peptide (BNP) mRNA levels 240 min after cyclic stretch of neonatal ventricular rat cardiomyocytes (Pikkarainen et al., 2003). Another study demonstrates that transforming growth factor β1 upregulation induced by acute (30 min) stretch is due to the

* Corresponding author. Al. Prof. Hernâni Monteiro, 4200-319, Porto, Portugal. Tel.: +351 22 5508452; fax: +351 22 5519194.

E-mail address: amoreira@med.up.pt (A.F. Leite-Moreira).

0024-3205/$ - see front matter © 2005 Elsevier Inc. All rights reserved.
doi:10.1016/j.lfs.2005.10.021

paracrine action of pre-formed angiotensin II and endothelin 1 (ET-1) (Malhorta et al., 1999). Interestingly, the type of mechanical stimulus seems to be determinant for the pattern of molecular adaptation. Yamamoto et al. showed p44/42 MAPK and MEK1/2 activation by cyclic systolic stress, but not by tension selectively applied in the last third of the cardiac cycle (Yamamoto et al., 2001).

In the intact heart, acute pressure and volume overload induced different local growth factor formation (Modesti et al., 2000). This was associated with distinct hemodynamics and specific patterns of ventricular remodeling (concentric vs. eccentric hypertrophy) (Modesti et al., 2000, 2004).

Given that early changes of myocardial gene expression might underlie ventricular remodeling subsequent to hemodynamic stress we investigated, in acute volume and RV pressure overload, the activation of genes previously implicated in myocardial hypertrophy and contractile dysfunction. Specifically, we evaluated and correlated biventricular hemodynamics and myocardial mRNA levels of BNP, pro-inflammatory cytokines (IL-6 and TNF-α), iNOS, growth factors (IGF-1, ppET-1), ACE and the Ca^{2+}-handling proteins SERCA2a, phospholamban (PLB) and calsequestrin (CSQ), after 120 and 360 min of volume overload or selective RV pressure overload, in the in situ rat heart.

Materials and methods

Experimental design

Animal experiments were performed according to the Portuguese law on animal welfare and conform to the National Institutes of Health Guide for the Care and Use of Laboratory Animals (NIH. Pub. No. 85-23, Revised 1996). Eight weeks old adult male Wistar rats ($n=45$; Charles River Laboratories; Barcelona, Spain) were housed in groups of 5 rats/cage in a controlled environment under 12:12 h light–dark cycle at a room temperature of 22 °C, with a free supply of food and water.

Rats were randomly assigned to one of three protocols: i) RV acute pressure overload (P-Band) induced by pulmonary trunk banding in order to double RV peak systolic pressure (RVP_{max}), during 120 ($n=7$) or 360 ($n=8$) min; ii) acute volume overload (Dextran) induced by dextran40 infusion (5 ml/h), during 120 ($n=8$) or 360 ($n=9$) min; iii) sham groups of 120 ($n=7$) and 360 ($n=6$) min. The mortality rate was 13.3% in P-Band (2 animals in the 360 min protocol) and 23.5% in dextran (1 animal in the 120 min protocol and 3 animals in the 360 min protocol). No deaths occurred in Sham.

After hemodynamic instrumentation the animals were euthanized with anesthetic overdose and transmural RV and LV free-wall samples were collected and snap frozen in liquid nitrogen, being stored at −70 °C for mRNA quantification.

Hemodynamic studies

The animals were anesthetized with pentobarbital (6 mg/100 g, ip), placed over a heating pad, and tracheostomized for mechanical ventilation with oxygen-enriched air at 60 cpm, with a tidal volume of 1 ml/100 g (Harvard Small Animal Ventilator, model 683). Respiratory rate and tidal volume were adjusted to keep arterial blood gases and pH within physiological limits. Anesthesia was maintained with an additional bolus of pentobarbital (2 mg/100 g) as needed. The right jugular vein was cannulated, under binocular surgical microscopy (Wild M651.MS-D, Leica; Herbrugg, Switzerland), for fluid administration (prewarmed 0.9% NaCl solution) to compensate for perioperative fluid losses. The heart was exposed through a median sternotomy, and the pericardium was widely opened. Pulmonary trunk was dissected and a silk number 1 was passed around it. RV and LV pressures were measured with a 2-Fr high-fidelity micromanometer (SPR-324, Millar Instruments) inserted through the RV free-wall into the RV cavity and through an apical puncture wound into the LV cavity. After complete instrumentation, the animal preparation was allowed to stabilize for 15 min before the beginning of the experimental protocols. Hemodynamic recordings were made with respiration suspended at end-expiration. Parameters were converted on-line to digital data with a sampling frequency of 1 kHz. RV and LV pressure were measured at end-diastole (RVEDP and LVEDP, respectively) and peak systole (RVP_{max} and LVP_{max}). Peak rates of RV and LV pressure rise (dP/dt_{max}) and pressure fall (dP/dt_{min}) were measured as well. The relaxation rate was estimated with the time constant τ by fitting the isovolumetric pressure fall to a monoexponential function.

mRNA Quantification by real-time RT-PCR

Total mRNA was extracted through the guanidium-thiocyanate selective silica-gel membrane-binding method (Qiagen 74124) according to the manufacturer's instructions. Concentration and purity were assayed by spectrophotometry (Eppendorf 6131000.012).

Two-step real-time RT-PCR was used to perform relative quantification of mRNA, as previously described (Henriques-Coelho et al., 2004). For each studied mRNA molecule, standard curves were generated from the correlation between the amount of starting total mRNA and PCR threshold cycle (second derivative maximum method) of graded dilutions from a randomly selected tissue sample ($r>0.97$). For relative quantification of specific mRNA levels, 50 ng of total mRNA from each sample underwent two-step real-time RT-PCR. A melt curve analysis of each real-time PCR and 2% agarose gels (0.5 μg/ml ethidium bromide) were performed to exclude primer-dimer formation and assess the purity of the amplification product. The GAPDH mRNA level was similar in all experimental groups and was used as an internal control gene. Results of mRNA quantification are expressed in an arbitrary unit (AU) set as the average value of the sham group (sham=1 AU), after normalization for GAPDH.

RT (10 min at 22 °C, 50 min at 50 °C and 10 min at 95 °C) was performed in a standard thermocycler (Whatman Biometra 050-901) with a total volume of 20 μl:40 U/reaction of reverse transcriptase (Invitrogen 18064-014), 20

Table 1
Primers used in mRNA quantification by real-time RT-PCR

Gene	Primers 5′→3′	PCR amplicon (base pairs)
GAPDH	fw: TGGCCTTCCGTGTTCCTACCC rev: CCGCCTGCTTCACCACCTTCT	114
BNP	fw: GGACCAAGGCCCTACAAAAGA rev: CAGAGCTGGGGAAAGAAGAG	245
IGF-1	fw: CAGACGGGCATTGTGGAT rev: AGTCTTGGGCATGTCAGTGTG	114
ACE	fw: GCAGGCCAGCAGGGTCCACTACAC rev: GACCTCGCCATTCCGCTGATTCT	196
ppET-1	fw: CCATGCAGAAAGGCGTAAAAG rev: CGGGGCTCTGTAGTCAATGTG	198
TNF-α	fw: GGGGGCCTCCAGAACTCCA rev: TGGGCTACGGGCTTGTCA	216
IL-6	fw: CCGTTTCTACCTGGAGTTTG rev: GAAGTTGGGGTAGGAAGGAC	130
iNOS	fw: CCCAGCCCAACAACACAGGAT rev: GGGCGGGTCGATGGAGTCA	112
SERCA2a	fw: CGAGTTGAACCTTCCCACAA rev: GGAGGAGATGAGGTAGCGGATGGA	240
PLB	fw: GGCATCATGGAAAAAGTCCA rev: GGTGGAGGGCCAGGTTGTAA	224
CSQ	fw: AGCAGCGTCTCCAAGAA rev: CGTGGTAGTAGAGACAGAGCAAA	248

U/reaction of RNase inhibitor (Promega N2515), 30 ng/ml random primers (Invitrogen 48190-011), 0.5 mM nucleotide mix (MBI Fermentas R0192), 1.9 mM $MgCl_2$ and 10 mM DTT. Ten percent of the cDNA yield was used as a template for real-time PCR (LightCycler, Roche) using SYBR green (Qiagen 204143) according to the manufacturer's instructions. Specific PCR primer pairs for the studied genes are presented in Table 1.

Statistical analysis

Data are presented as mean ± SEM. Hemodynamic data were compared using two-way repeated measures ANOVA. Differences in mRNA expression between experimental groups were analyzed by one-way ANOVA (for normally distributed data) or by the corresponding non-parametric test (Kruskal–Wallis ANOVA on Ranks). Linear regression and Pearson correlation coefficients were employed to correlate variables. When necessary, the test was preceded by a square root transform to obtain a normal distribution. Statistical significance was set at $P<0.05$.

Results

Biventricular hemodynamics in acute cardiac overload

Acute pulmonary banding and dextran infusion induced distinct hemodynamic responses. Pulmonary banding (Table 2) induced a selective pressure overload of the RV, with no significant changes in LV hemodynamics. Pulmonary trunk was constricted until basal RVP_{max} was doubled. This was accompanied by an augmentation of RV-dP/dt_{max} and slower relaxation as denoted by the prolongation of the RV time constant τ. RVEDP increased significantly at 240 and 300 min. On the other hand, acute intravascular volume expansion with dextran (Table 3) progressively increased EDP and τ in both ventricles, while P_{max} was selectively increased in the RV.

Hemodynamics of sham operated animals remained unaltered throughout the experimental protocol (Table 4). Heart rate was similar in all the studied groups (298 ± 8.9 bpm) and did not vary during the experimental protocols. Biventricular hemodynamic data from the animals euthanized at 120 min were similar to their counterparts euthanized at 360 min, and therefore are not presented.

Biventricular gene expression profile in acute cardiac overload

Myocardial gene expression profile was distinct in P-Band and Dextran groups. BNP was upregulated at 360 min in the overloaded ventricles (Fig. 1). In fact, both pulmonary banding and dextran infusion raised BNP mRNA levels in the RV, while only dextran infusion modified BNP expression in the LV. Unexpectedly, we observed BNP downregulation in the LV after 120 min of dextran infusion, which reversed at 360 min.

Table 2
RV and LV hemodynamics during acute pulmonary trunk banding

Pulmonary Banding	0 min	60 min	120 min	180 min	240 min	300 min	360 min
RV							
$RVP_{max,\ mm\ Hg}$	24.3 ± 1.0	54.1 ± 2.7*$^{\dagger\delta}$	55.1 ± 4.1*$^{\dagger\delta}$	54.2 ± 4.1*$^{\dagger\delta}$	56.3 ± 3.9*$^{\dagger\delta}$	50.0 ± 5.2*$^{\dagger\delta}$	49.2 ± 4.6*†
$dP/dt_{max,\ mm\ Hg/s}$	1076 ± 74	2097 ± 128*	2214 ± 318*	2146 ± 287*	2141 ± 227*	1906 ± 255*	1862 ± 287*
$dP/dt_{min,\ mm\ Hg/s}$	−730 ± 58	−1199 ± 128	−1174 ± 154	−1100 ± 142	−1057 ± 110	−1022 ± 103	−1000 ± 147
$RVEDP_{,\ mm\ Hg}$	0.6 ± 0.3	2.2 ± 1.0	3.5 ± 0.8	4.0 ± 0.6	5.0 ± 0.9*	4.5 ± 1.1*	4.3 ± 1.2*
τ, ms	10.6 ± 1.2	15.6 ± 1.4*	15.8 ± 1.8*	17.2 ± 1.5*	17.2 ± 1.3*	17.5 ± 1.3*	16.8 ± 1.0*
LV							
$LVP_{max,\ mm\ Hg}$	91.0 ± 5.3	86.6 ± 4.0	88.3 ± 3.6	90.7 ± 3.1	90.0 ± 1.9	90.0 ± 2.8	82.2 ± 4.2
$dP/dt_{max,\ mm\ Hg/s}$	5531 ± 964	5132 ± 436	5556 ± 675	5551 ± 729	5834 ± 488	5619 ± 658	4894 ± 746
$dP/dt_{min,\ mm\ Hg/s}$	−4104 ± 575	−3588 ± 327	−3590 ± 360	−3212 ± 299	−3231 ± 286	−3233 ± 234	−2798 ± 308
$LVEDP_{,\ mm\ Hg}$	1.8 ± 0.4	2.4 ± 0.7	3.2 ± 0.4$^{\delta}$	3.5 ± 0.4$^{\delta}$	3.5 ± 0.4$^{\delta}$	3.1 ± 0.3$^{\delta}$	3.7 ± 0.7$^{\delta}$
τ, ms	16.1 ± 1.3	15.1 ± 1.1	15.3 ± 0.8	16.8 ± 1.2	17.3 ± 1.2	17.2 ± 1.0$^{\delta}$	16.9 ± 0.7$^{\delta}$

Data are mean ± SE. RVP_{max} and LVP_{max}, RV and LV peak systolic pressures, respectively; dP/dt_{max} and dP/dt_{min}, peak rates of ventricular pressure rise and fall, respectively; RVEDP and LVEDP, RV and LV end-diastolic pressures, respectively; τ, time constant of isovolumetric relaxation; *$P<.05$ vs. 0′; $^{\dagger}P<0.05$ vs. sham; $^{\delta}P<0.05$ vs. dextran infusion.

Table 3
RV and LV hemodynamics during dextran e.v. infusion

Dextran40	0 min	60 min	120 min	180 min	240 min	300 min	360 min
RV							
$RVP_{max,\ mm\ Hg}$	25.9±1.0	27.7±1.2$^{\delta}$	32.1±2.1$^{\delta}$	34.8±2.5*$^{\delta}$	40.4±2.3*$^{\delta}$	40.9±2.7*$^{\delta}$	42.4±3.3*
$dP/dt_{max,\ mm\ Hg/s}$	1032±79	1230±108	1224±143	1282±152	1306±151	1261±149	1318±166
$dP/dt_{min,\ mm\ Hg/s}$	−833±138	−1160±154	−1162±149	−1125±157	−1241±166	−984±141	−999±153
RVEDP, $_{mm\ Hg}$	1.1±0.6	1.3±1.0	4.0±1.1	5.0±1.5*	7.2±2.3*†	6.9±2.2*	6.9±2.5*
τ, ms	12.2±0.8	13.0±1.0	14.5±1.5	15.5±1.3	16.5±1.8*	18.3±1.6*	19.7±1.8*
LV							
$LVP_{max,\ mm\ Hg}$	97.8±7.9	108.4±6.2	109.2±8.5	102.5±9.3	101.5±6.9	81.6±7.1	81.4±7.0
$dP/dt_{max,\ mm\ Hg/s}$	4614±567	6625±787	6433±901	5718±740	5370±709	3863±480	3824±499
$dP/dt_{min,\ mm\ Hg/s}$	−3714±465	−4543±601	−4162±572	−3684±553	−3432±377	−2398±387	−2409±396
LVEDP, $_{mm\ Hg}$	3.0±1.2	5.7±2.4*	6.7±1.5*$^{\dagger\delta}$	7.3±1.6*$^{\dagger\delta}$	7.9±2.3*$^{\dagger\delta}$	6.2±1.7*$^{\delta}$	5.9±1.8*$^{\delta}$
τ, ms	14.4±0.3	16.2±0.6	17.9±1.2*	19.3±2.0*	21.0±1.5*	22.2±1.2*$^{\dagger\delta}$	23.0±1.1*$^{\dagger\delta}$

Data are mean±SE. RVP_{max} and LVP_{max}, RV and LV peak systolic pressures, respectively; dP/dt_{max} and dP/dt_{min}, peak rates of ventricular pressure rise and fall, respectively; RVEDP and LVEDP, RV and LV end-diastolic pressures, respectively; τ, time constant of isovolumetric relaxation; *$P<.05$ vs. 0′; $^{\dagger}P<0.05$ vs. Sham; $^{\delta}P<0.05$ vs. pulmonary trunk banding.

Acute cardiac overload also affected myocardial growth factor expression (Fig. 1). In the RV we observed IGF-1 upregulation at 360 min, similar in Dextran and P-Band groups. Regarding ppET-1, there was a pronounced upregulation of its myocardial expression 360 min after dextran infusion, both in RV and LV, whilst pulmonary trunk banding promoted a lower increase of ppET-1 mRNA levels restricted to the RV. We did not detect changes in myocardial expression of ACE.

Myocardial gene activation of IL-6 and TNF-α was higher in volume than in pressure overload (Fig. 2). It should be noted that TNF-α upregulation was also observed at 360 min in the non-overloaded LV of P-Band. Accordingly, a strong positive correlation between RV and LV mRNA levels of TNF-α ($r=0.81$; $p<0.0001$) was observed in all experimental protocols. We did not detect changes in iNOS myocardial expression.

Regarding the myocardial expression of Ca^{2+}-handling proteins (Fig. 3), SERCA2a and PLB were upregulated in the RV after 360 min of dextran infusion, while pulmonary trunk banding did not significantly change mRNA levels of these genes. SERCA2a overexpression was also present in the LV at 360 min of Dextran group. CSQ, assayed as a possible internal control gene, varied significantly from Sham both in P-Band and Dextran.

Correlation of gene expression with end-diastolic and peak systolic pressures

mRNA levels of BNP, TNF-α and SERCA2a in the RV selectively correlate with RVEDP, but not with RVP_{max}, in all experimental groups (Fig. 4). For IGF-1, ppET-1 and IL-6, positive correlations were found between RV mRNA levels and both RVEDP and RVP_{max} (Fig. 5).

Dextran infusion elevated EDP and altered myocardial gene expression in both ventricles. In this experimental protocol, significant correlations were observed between RV and LV mRNA levels of the following genes: BNP ($r=0.49$; $p=0.018$), ppET-1 ($r=0.75$; $p=0.0002$), TNF-α ($r=0.77$; $p<0.0001$), IL-6 ($r=0.83$; $p<0.0001$) and SERCA2a ($r=0.67$; $p=0.0006$). In this experimental protocol, PLB and IGF-1 upregulation was restricted to the RV. For these two genes, expression levels

Table 4
RV and LV hemodynamics in sham

Sham	0 min	60 min	120 min	180 min	240 min	300 min	360 min
RV							
$RVP_{max,\ mm\ Hg}$	27.0±1.6	27.2±1.9	26.4±1.7	28.5±2.2	30.8±2.0	30.7±1.8	29.9±2.0
$dP/dt_{max,\ mm\ Hg/s}$	1460±126	1462±193	1471±213	1445±213	1486±179	1473±174	1437±234
$dP/dt_{min,\ mm\ Hg/s}$	−985±148	−1021±214	−1033±199	−1073±193	−1227±134	−1316±177	−1316±189
RVEDP, $_{mm\ Hg}$	1.7±0.9	3.0±1.1	2.5±0.9	2.1±0.8	2.4±0.7	2.5±0.8	2.7±1.1
τ, ms	12.3±0.9	13.1±0.6	13.1±0.8	12.9±0.9	13.1±1.1	13.5±0.8	14.0±1.2
LV							
$LVP_{max,\ mm\ Hg}$	95.5±6.0	102±9.1	96.0±10.2	95.7±9.3	95.1±6.9	92.1±6.3	92.2±6.8
$dP/dt_{max,\ mm\ Hg/s}$	5517±658	6675±1002	6201±1130	5860±918	5637±399	5622±419	5339±419
$dP/dt_{min,\ mm\ Hg/s}$	−3905±301	−4718±601	−4322±743	−4140±570	−3926±419	−3663±358	−3348±252
LVEDP, mm Hg	2.4±0.4	2.5±0.5	2.7±0.7	3.0±0.8	3.2±0.3	3.5±0.4	3.9±0.5
τ, ms	15.6±0.6	15.3±0.4	15.6±0.6	15.8±0.6	16.1±0.6	16.1±0.7	16.6±0.6

Data are mean±SE. RVP_{max} and LVP_{max}, RV and LV peak systolic pressures, respectively; dP/dt_{max} and dP/dt_{min}, peak rates of ventricular pressure rise and fall, respectively; RVEDP and LVEDP, RV and LV end-diastolic pressures, respectively; τ, time constant of isovolumetric relaxation.

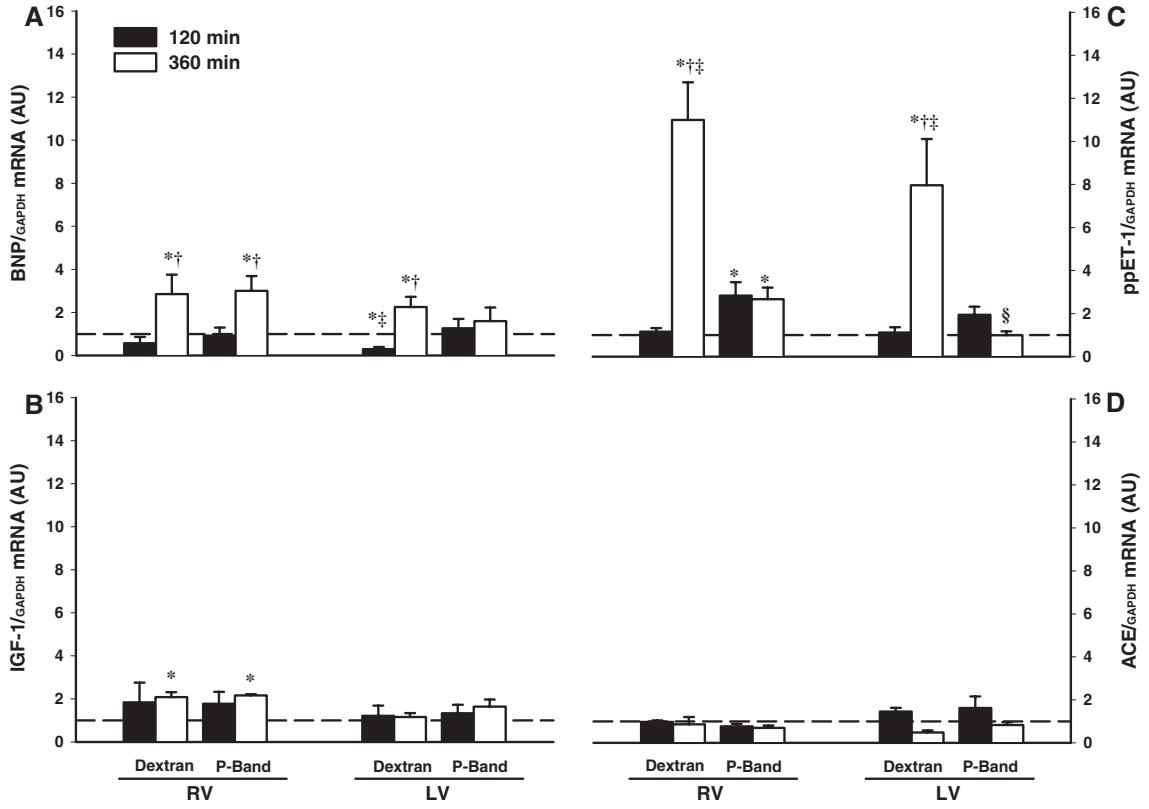

Fig. 1. Biventricular expression of BNP (A), IGF-1 (B), ppET-1 (C) and ACE (D), 120 and 360 min after dextran infusion (Dextran) or pulmonary trunk banding (P-Band). Results are presented in arbitrary units (sham = 1 AU). *$P<0.05$ vs. Sham; †$P<0.05$ vs. 120 min; ‡$P<0.05$ vs. P-Band; §$P<0.05$ vs. RV.

positively correlated with RVP_{max} (PLB: $r=0.60$, $p=0.0019$; IGF-1: $r=0.67$, $p=0.0004$).

Discussion

In the present study we demonstrate acute modulation of gene expression, as early as 120 min, after volume and RV pressure overload in the in situ rat heart. This modulation encompassed BNP, growth factors, pro-inflammatory cytokines, Ca^{2+}-handling proteins, and although it mainly involved the overloaded ventricles, it also affected the non-overloaded myocardium. Changes in myocardial gene expression correlated with systolic and diastolic pressures and were distinct in volume and pressure overload.

Dextran infusion induced a progressive increase of EDP and τ in both ventricles, which was accompanied by concurrent upregulation of BNP, ppET-1, TNF-α, IL-6 and SERCA2a in RV and LV. P_{max} elevation, however, was restricted to the RV, a feature also observed in the aorta-cava fistula model (Modesti et al., 2004). The selective increase of PLB and IGF-1 mRNA in the RV could indicate that, in the setting of a volume overload, some degree of concomitant pressure overload might be required for the upregulation of these genes.

In our study, TNF-α gene activation was present in the overloaded ventricles, in accordance with the results of previous reports (Baumgarten et al., 2002; Kapadia et al., 1997). However, TNF-α was not upregulated in chronic pressure (Baumgarten et al., 2002) and volume (Dai et al., 2004) overload, despite persistent hemodynamic stress. It was suggested that sustained cardiac overload could induce the activation of tristetraprolin, a zinc protein which destabilize TNF-α mRNA in various cell types (Baumgarten et al., 2002; Dai et al., 2004).

Interestingly, we observed TNF-α upregulation in the nonoverloaded LV of rats subjected to pulmonary trunk banding indicating gene activation by load-independent mechanisms, most likely paracrine or endocrine mediation. In fact, TNF-α upregulation in the infarcted myocardium induces cytokine upregulation in the neighbouring myocardium (Nian et al., 2004) and early post-ischemic cardiac lymph activates cytokine expression in canine mononuclear cells, an effect that is lost after incubation with a neutralizing antibody to TNF-α (Frangogiannis et al., 2002). Moreover, TNF-α is induced in the normal recipient heart of rats after heterotopic post-myocardial infarct heart transplants (Nakamura et al., 2003).

The pattern of gene response for TNF-α was not mimicked by IL-6. IL-6 activation was restricted to the overloaded ventricles, with no gene activation in the LV of P-Band. Although TNF-α is a well-accepted upstream cytokine inducing IL-6 gene activation, our results suggest that, in the absence of myocardial overload, acute upregulation of the former is not accompanied by overexpression of the latter. This might not be surprising since IL-6 upregulation was already observed in chronic volume overload in the absence of concomitant TNF-α activation (Dai et al., 2004), further dissociating the expression of these two genes.

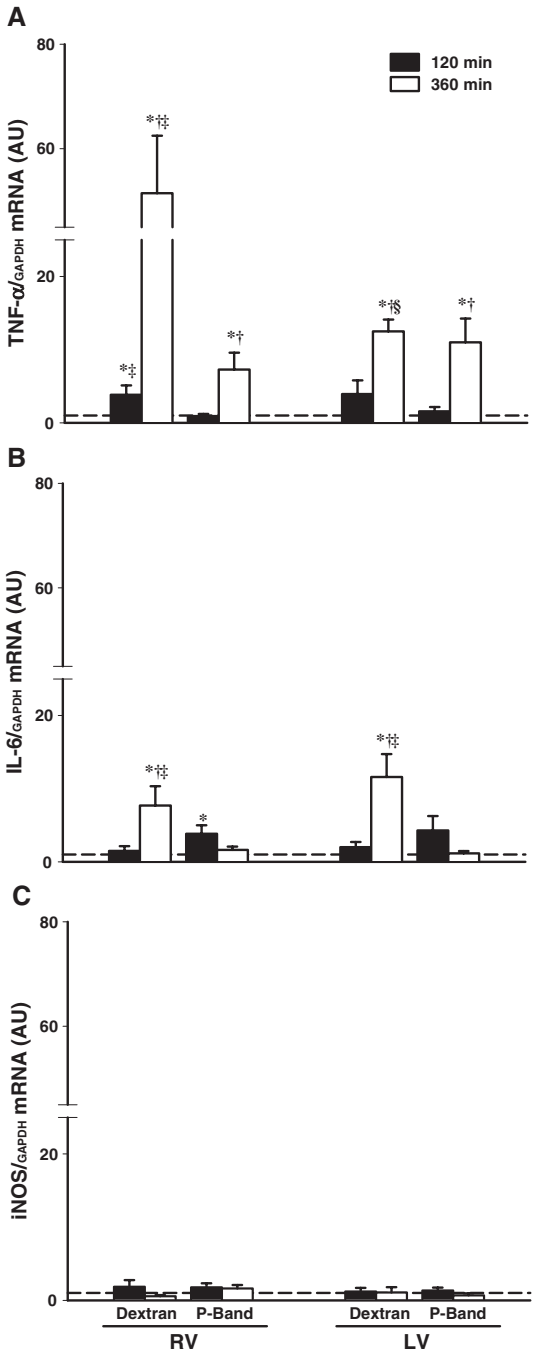

Fig. 2. Biventricular expression of TNF-α (A), IL-6 (B), and iNOS (C), 120 and 360 min after dextran infusion (Dextran) or pulmonary trunk banding (P-Band). Results are presented in arbitrary units (sham=1 AU). *$P<0.05$ vs. Sham; †$P<0.05$ vs. 120 min; ‡$P<0.05$ vs. P-Band; §$P<0.05$ vs. RV.

Acute upregulation of IL-6 and TNF-α was more pronounced with volume than with pressure overload. Interestingly, these cytokines have been implicated in the development of the eccentric hypertrophy phenotype. Transgenic mice with cardiac restricted overexpression of TNF-α present progressive LV dilation (Sivasubramanian et al., 2001), and the activation of IL-6 receptor transmembranar domain gp130 in isolated neonatal rat cardiomyocytes induces sarcomere longitudinal growth (Wollert et al., 1996).

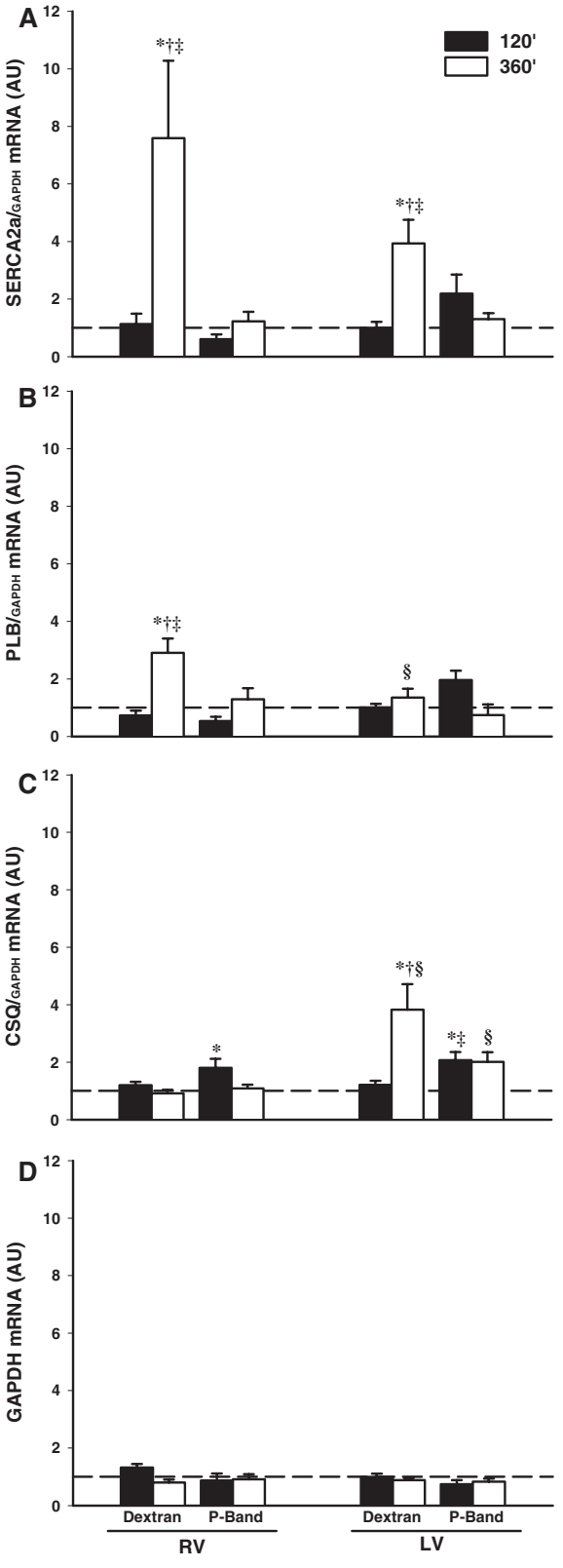

Fig. 3. Biventricular expression of SERCA2a (A), phospholamban (PLB;B), calsequestrin (CSQ;C) and GAPDH (D), 120 and 360 min after dextran infusion (Dextran) or pulmonary trunk banding (P-Band). Results are presented in arbitrary units (sham=1 AU). *$P<0.05$ vs. Sham; †$P<0.05$ vs. 120 min; ‡$P<0.05$ vs. P-Band; §$P<0.05$ vs. RV.

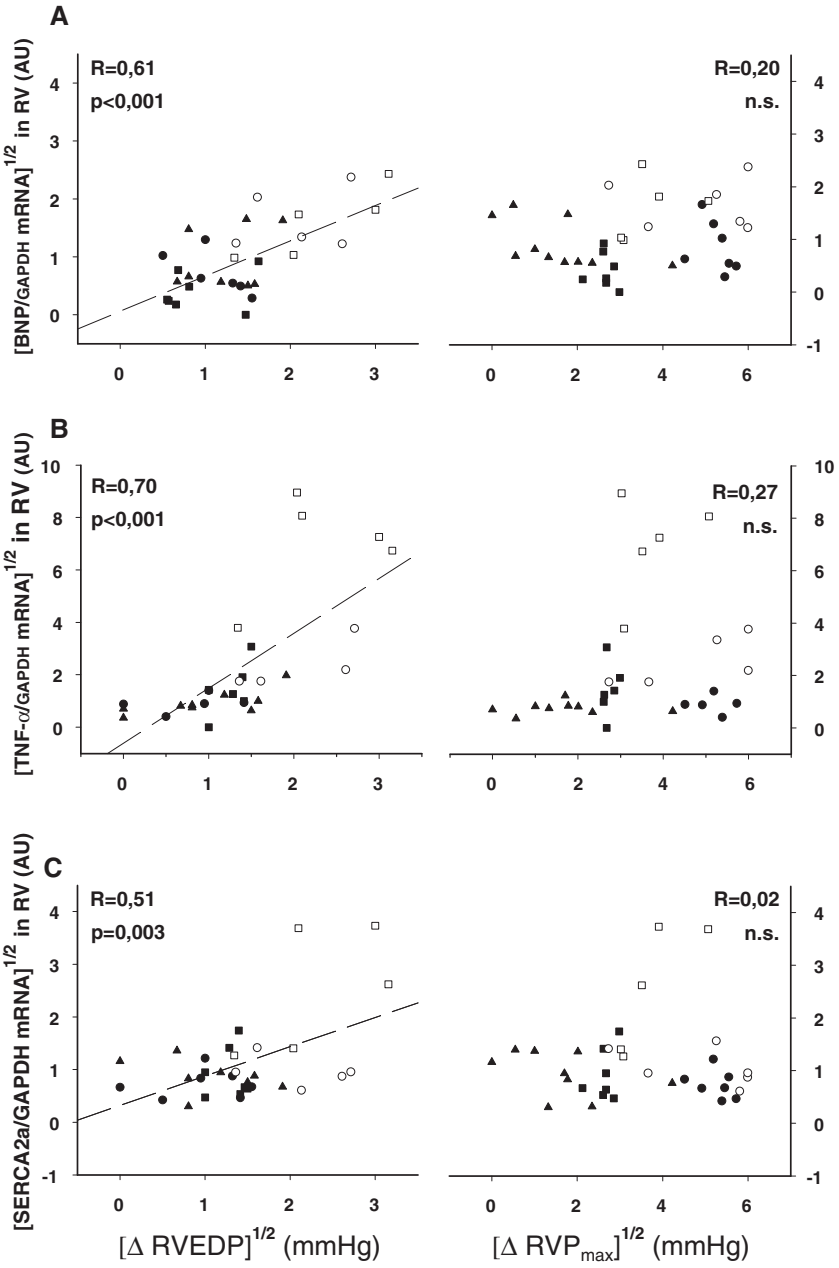

Fig. 4. Correlations between RV end-diastolic pressure (left panels) and RV peak-systolic pressure (right panels) with mRNA levels of BNP (A), TNF-α (B) and SERCA2a (C) in Sham (▲), P-Band 120 (●) and 360 min (○), and Dextran 120 (■) and 360 min (□) groups, in the RV. The hemodynamic parameters were expressed as the difference between the value at 120 or 360 min, and the basal value at the beginning of the experimental protocol. Square root transforms were performed to obtain normal distributions. mRNA levels are presented in arbitrary units (sham=1 AU).

RV IGF-1 overexpression in P-Band was similar to Dextran, in accordance with previous studies showing an upregulation of this gene in pressure and volume overload (Modesti et al., 2000, 2004). Given its pro-hypertrophic and anti-apoptotic actions, IGF-1 might contribute to myocardial adaptation to cardiac overload (Tanaka et al., 1998; Welch et al., 2002). Differently, dextran infusion induced a higher increase of ppET-1 expression than pulmonary trunk banding. This somewhat diverges from what was previously described for distinct types of acute LV overload (Modesti et al., 2000). In this study, only acute aortic banding induced ppET-1 upregulation, with no differences detected in the aorto-caval fistula group. This could depend on the distinct features of RV and LV, as well as on the mixed pressure–volume load faced by the RV after dextran infusion. The mixed pressure–volume load to which the RV is subjected has also been proposed to explain selective RV ppET-1 activation in chronic volume overload (Modesti et al., 2004).

Natriuretic peptide upregulation after mechanical and pharmacological stimulation is used as a molecular marker of cardiac hypertrophic gene response (van Wamel et al., 2000), and represents a regression to the molecular fetal phenotype (Takahashi et al., 1992). The present study shows increased BNP mRNA levels in acute pressure and volume overloaded

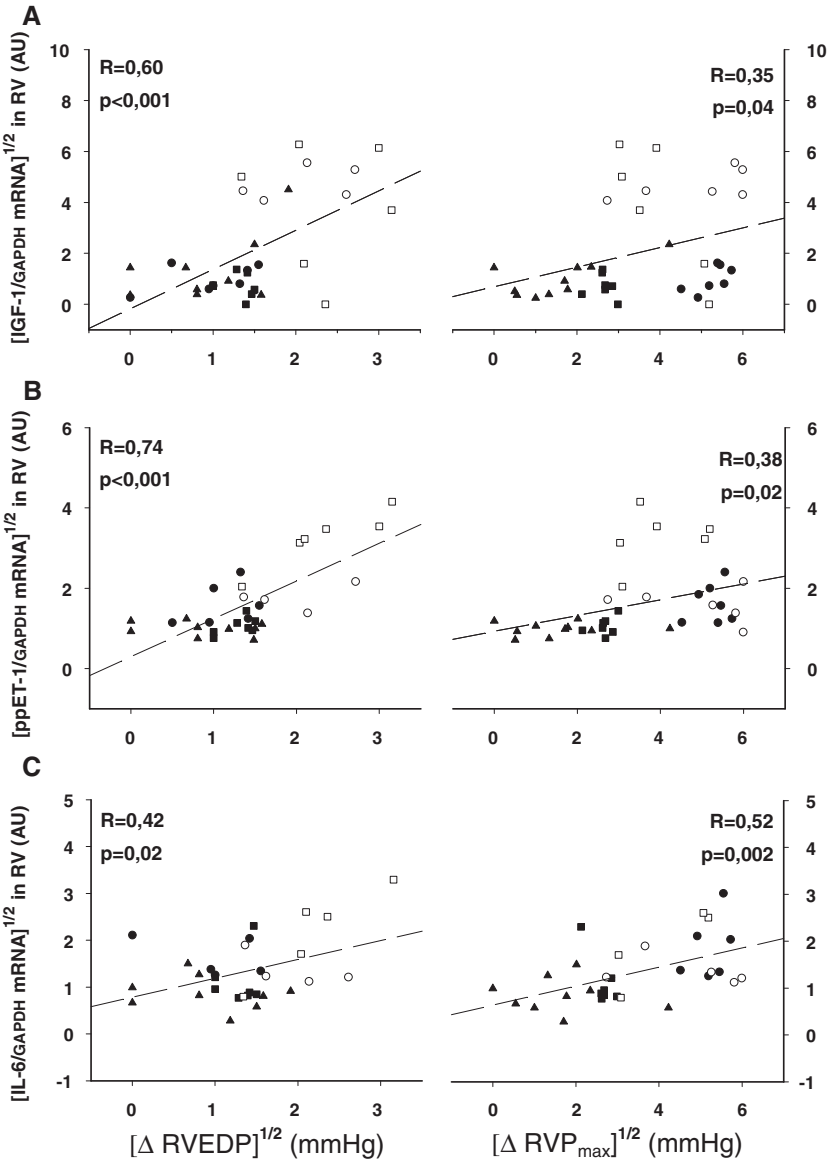

Fig. 5. Correlations between RV end-diastolic pressure (left panels) and RV peak-systolic pressure (right panels) with mRNA levels of IGF-1 (A), ppET-1 (B) and IL-6 (B) in Sham (▲), P-Band 120 (●) and 360 min (○), and Dextran 120 (■) and 360 min (□) groups, in the RV. The hemodynamic parameters were expressed as the difference between the value at 120 or 360 min, and the basal value at the beginning of the experimental protocol. Square root transforms were performed to obtain normal distributions. mRNA levels are presented in arbitrary units (sham=1 AU).

ventricles. Previous studies addressing this issue were carried out in the isolated rat heart (Magga et al., 1997) or in neonatal rat ventricular cardiomyocytes (van Wamel et al., 2000).

Impaired cardiomyocyte Ca^{2+}-handling has been implicated in the origin of contractile dysfunction during heart failure progression (Bers, 2002). Decreased expression of the major Ca^{2+}-handling protein SERCA2a (Hasenfuss et al., 1994) and enhanced inhibition by its major regulator PLB have been demonstrated in advanced heart failure (Sande et al., 2002). Despite extensive evidence for altered expression of Ca^{2+}-handling proteins in heart failure, the acute response to cardiac overload remains unknown. To our knowledge, the present study is the first to demonstrate SERCA2a and PLB upregulation by acute volume overload, in vivo. Unlike what has been described in chronic overload, with decreased SERCA2a expression in both pressure (Feldman et al., 1993) and volume overload (Nediani et al., 2002), a different response in acute pulmonary banding and dextran infusion was observed, with SERCA2a upregulation restricted to the latter. This early upregulation would fit in a model of biphasic expression of these genes during the time course of adaptation to volume overload. Myocardial expression of the major Ca^{2+}-binding protein of the sarcoplasmic reticulum CSQ was also altered in acute cardiac overload. This diverges from the stable mRNA levels observed in heart failure, with differences detected only at the post-translational level (Kiarash et al., 2004).

Previous works showed that acute mechanical stretch modulates cardiomyocyte gene expression in vitro (Palmieri et al., 2002; van Wamel et al., 2000). In our study, we found significant in vivo correlations between myocardial mRNA

levels of several genes and both diastolic and systolic pressures, although the number and strength of these correlations were higher with the former. Since the studied genes have been implicated in myocardial function and remodeling, it is plausible that different patterns of gene expression in acute cardiac overload might underlie distinct functional and hypertrophic phenotypes in chronic pressure and volume overload.

Acronyms

ACE Angiotensin converting enzyme
BNP Type B natriuretic peptide
CSQ Calsequestrin
dP/dt_{max} Peak rate of pressure rise
dP/dt_{min} Peak rate of pressure fall
GAPDH Glyceraldehyde-3-phosphate dehydrogenase
IGF-1 Insulin-like growth factor 1
IL-6 Interleukin 6
iNOS Inducible nitric oxide synthase
LV Left ventricle or left ventricular
LVEDP LV end-diastolic pressure
LVP_{max} Peak systolic LV pressure
P-Band Pulmonary trunk banding
PLB Phospholamban
ppET-1 Pre-pro-endothelin 1
RV Right ventricle or right ventricular
RVEDP RV end-diastolic pressure
RVP_{max} Peak systolic RV pressure
SERCA2a Sarcoplasmic reticulum Ca^{2+} ATPase
τ Time constant of isovolumetric relaxation
TNF-α Tumour necrosis factor alpha

Acknowledgments

Supported by grants from 'Fundação para a Ciência e Tecnologia' (POCTI/CBO/47519/02; partially funded by Fundo Europeu de Desenvolvimento Regional) and from 'Cardiovascular R&D Unit' (51/94-FCT, Portugal).

References

Baumgarten, G., Knuefermann, P., Kalra, D., Gao, F., Taffet, G.E., Michael, L., Blackshear, P.J., Carballo, E., Sivasubramanian, N., Mann, D.L., 2002. Load-dependent and -independent regulation of proinflammatory cytokine and cytokine receptor gene expression in the adult mammalian heart. Circulation 105, 2192–2197.

Bers, D.M., 2002. Cardiac excitation–contraction coupling. Nature 415, 198–205.

Dai, R.P., Dheen, S.T., He, B.P., Tay, S.S., 2004. Differential expression of cytokines in the rat heart in response to sustained volume overload. European Journal of Heart Failure 6, 693–703.

Feldman, A.M., Weinberg, E.O., Ray, P.E., Lorell, B.H., 1993. Selective changes in cardiac gene expression during compensated hypertrophy and the transition to cardiac decompensation in rats with chronic aortic banding. Circulation Research 73, 184–192.

Frangogiannis, N.G., Smith, C.W., Entman, M.L., 2002. The inflammatory response in myocardial infarction. Cardiovascular Research 53, 31–47.

Hasenfuss, G., Reinecke, H., Studer, R., Meyer, M., Pieske, B., Holtz, J., Holubarsch, C., Posival, H., Just, H., Drexler, H., 1994. Relation between myocardial function and expression of sarcoplasmic reticulum Ca(2+)-ATPase in failing and nonfailing human myocardium. Circulation Research 75, 434–442.

Henriques-Coelho, T., Correia-Pinto, J., Roncon-Albuquerque Jr., R., Baptista, M.J., Lourenco, A.P., Oliveira, S.M., Brandao-Nogueira, A., Teles, A., Fortunato, J.M., Leite-Moreira, A.F., 2004. Endogenous production of ghrelin and beneficial effects of its exogenous administration in monocrotaline-induced pulmonary hypertension. American Journal of Physiology. Heart and Circulatory Physiology 287, H2885–H2890.

Hoshijima, M., Chien, K.R., 2002. Mixed signals in heart failure: cancer rules. Journal of Clinical Investigation 109, 849–855.

Kapadia, S.R., Oral, H., Lee, J., Nakano, M., Taffet, G.E., Mann, D.L., 1997. Hemodynamic regulation of tumor necrosis factor-alpha gene and protein expression in adult feline myocardium. Circulation Research 81, 187–195.

Kiarash, A., Kelly, C.E., Phinney, B.S., Valdivia, H.H., Abrams, J., Cala, S.E., 2004. Defective glycosylation of calsequestrin in heart failure. Cardiovascular Research 63, 264–272.

Magga, J., Vuolteenaho, O., Tokola, H., Marttila, M., Ruskoaho, H., 1997. Involvement of transcriptional and posttranscriptional mechanisms in cardiac overload-induced increase of B-type natriuretic peptide gene expression. Circulation Research 81, 694–702.

Malhorta, R., Sadoshima, J., Brosius III, F.C., Izumo, S., 1999. Mechanical stretch and angiotensin II differentially upregulate the rennin–angiotensin system in cardiac myocytes in vitro. Circulation 85, 137–146.

Modesti, P.A., Vanni, S., Bertolozzi, I., Cecioni, I., Polidori, G., Paniccia, R., Bandinelli, B., Perna, A., Liguori, P., Boddi, M., Galanti, G., Serneri, G.G., 2000. Early sequence of cardiac adaptations and growth factor formation in pressure- and volume-overload hypertrophy. American Journal of Physiology. Heart and Circulatory Physiology 279, H976–H985.

Modesti, P.A., Vanni, S., Bertolozzi, I., Cecioni, I., Lumachi, C., Perna, A.M., Boddi, M., Gensini, G.F., 2004. Different growth factor activation in the right and left ventricles in experimental volume overload. Hypertension 43, 101–108.

Morisco, C., Sadoshima, J., Trimarco, B., Arora, R., Vatner, D.E., Vatner, S.F., 2003. Is treating cardiac hypertrophy salutary or detrimental: the two faces of Janus. American Journal of Physiology. Heart and Circulatory Physiology 284, H1043–H1047.

Nakamura, H., Umemoto, S., Naik, G., Moe, G., Takata, S., Liu, P., Matsuzaki, M., 2003. Induction of left ventricular remodeling and dysfunction in the recipient heart after donor heart myocardial infarction: new insights into the pathologic role of tumor necrosis factor-alpha from a novel heterotopic transplant-coronary ligation rat model. Journal of the American College of Cardiology 42, 173–181.

Nediani, C., Formigli, L., Perna, A.M., Pacini, A., Ponziani, V., Modesti, P.A., Ibba-Manneschi, L., Zecchi-Orlandini, S., Fiorillo, C., Cecchi, C., Liguori, P., Fratini, G., Vanni, S., Nassi, P., 2002. Biochemical changes and their relationship with morphological and functional findings in pig heart subjected to lasting volume overload: a possible role of acylphosphatase in the regulation of sarcoplasmic reticulum calcium pump. Basic Research in Cardiology 97, 469–478.

Nian, M., Lee, P., Khaper, N., Liu, P., 2004. Inflammatory cytokines and postmyocardial infarction remodeling. Circulation Research 94, 1543–1553.

Palmieri, E.A., Benincasa, G., Di Rella, F., Casaburi, C., Monti, M.G., De Simone, G., Chiariotti, L., Palombini, L., Bruni, C.B., Sacca, L., Cittadini, A., 2002. Differential expression of TNF-alpha, IL-6, and IGF-1 by graded mechanical stress in normal rat myocardium. American Journal of Physiology. Heart and Circulatory Physiology 282, H926–H934.

Pikkarainen, S., Tokola, H., Majalahti-Palviainen, T., Kerkela, R., Hautala, N., Bhalla, S.S., Charron, F., Nemer, M., Vuolteenaho, O., Ruskoaho, H., 2003. GATA-4 is a nuclear mediator of mechanical stretch-activated hypertrophic program. Biological Chemistry 278, 23807–23816.

Sande, J.B., Sjaastad, I., Hoen, I.B., Bokenes, J., Tonnessen, T., Holt, E., Lunde, P.K., Christensen, G., 2002. Reduced level of serine(16) phosphorylated phospholamban in the failing rat myocardium: a major contributor to reduced SERCA2 activity. Cardiovascular Research 53, 382–391.

Sivasubramanian, N., Coker, M.L., Kurrelmeyer, K.M., MacLellan, W.R., DeMayo, F.J., Spinale, F.G., Mann, D.L., 2001. Left ventricular remodeling in transgenic mice with cardiac restricted overexpression of tumor necrosis factor. Circulation 104, 826–831.

Sussman, M.A., McCulloch, A., Borg, T.K., 2002. Dance band on the Titanic: biomechanical signaling in cardiac hypertrophy. Circulation Research 91, 888–898.

Takahashi, T., Allen, P.D., Izumo, S., 1992. Expression of A-, B-, and C-type natriuretic peptide genes in failing and developing human ventricles. Circulation Research 71, 9–17.

Tanaka, N., Ryoke, T., Hongo, M., Mao, L., Rockman, H.A., Clark, R.G., Ross Jr., J., 1998. Effects of growth hormone and IGF-I on cardiac hypertrophy and gene expression in mice. American Journal of Physiology 275, H393–H399.

van Wamel, A.J., Ruwhof, C., van der Valk-Kokshoorn, L.J., Schrier, P.I., van der Laarse, A., 2000. Rapid effects of stretched myocardial and vascular cells on gene expression of neonatal rat cardiomyocytes with emphasis on autocrine and paracrine mechanisms. Archives of Biochemistry and Biophysics 381, 67–73.

Welch, S., Plank, D., Witt, S., Glascock, B., Schaefer, E., Chimenti, S., Andreoli, A.M., Limana, F., Leri, A., Kajstura, J., Anversa, P., Sussman, M.A., 2002. Cardiac-specific IGF-1 expression attenuates dilated cardiomyopathy in tropomodulin-overexpressing transgenic mice. Circulation Research 90, 641–648.

Wollert, K.C., Taga, T., Saito, M., Narazaki, M., Kishimoto, T., Glembotski, C.C., Vernallis, A.B., Heath, J.K., Pennica, D., Wood, W.I., Chien, K.R., 1996. Cardiotrophin-1 activates a distinct form of cardiac muscle cell hypertrophy. Assembly of sarcomeric units in series VIA gp130/leukemia inhibitory factor receptor-dependent pathways. Journal of Biological Chemistry 271, 9535–9545.

Yamamoto, K., Dang, Q.N., Maeda, Y., Huang, H., Kelly, R.A., Lee, R.T., 2001. Regulation of cardiomyocyte mechanotransduction by the cardiac cycle. Circulation 103, 1459–1464.